polysaccharides

MDPI

Article

Structural and Thermal Characterization of Some Thermoplastic Starch Mixtures

Maria Daniela Stelescu [1], Ovidiu-Cristian Oprea [2,3,*], Maria Sonmez [1], Anton Ficai [2,3], Ludmila Motelica [2,3], Denisa Ficai [2,3], Mihai Georgescu [1] and Dana Florentina Gurau [1]

[1] National Research & Development Institute for Textiles and Leather–Division, Leather and Footwear Research Institute, 93 Ion Minulescu St., 031215 Bucharest, Romania; maria.stelescu@icpi.ro (M.D.S.); maria.sonmez@icpi.ro (M.S.); mihai.georgesku@yahoo.com (M.G.); danagurau84@gmail.com (D.F.G.)
[2] Faculty of Chemical Engineering and Biotechnologies, National University of Science and Technology POLITEHNICA Bucharest, 1-7 Polizu St., 011061 Bucharest, Romania; anton.ficai@upb.ro (A.F.); ludmila.motelica@upb.ro (L.M.); denisa.ficai@upb.ro (D.F.)
[3] Academy of Romanian Scientists, 3 Ilfov St., 050044 Bucharest, Romania
* Correspondence: ovidiu.oprea@upb.ro

Abstract: The paper presents the production of thermoplastic starch (TPS) mixtures using potato starch and two types of plasticizers: glycerol and sorbitol. The effects of plasticizers, citric acid, organically modified montmorillonite clay nanofiller (OMMT) and an additive based on ultrahigh molecular weight siloxane polymer on the structure and physical–mechanical and thermal properties of TPS samples were analysed. Starch mixtures plasticized with glycerol were obtained, where the starch/glycerol mass ratio was 70:30, as well as starch mixtures plasticized with glycerol and sorbitol, with a starch/glycerol/sorbitol mass ratio of 60:20:20. The starch gelatinization process to obtain TPS was carried out in a Brabender Plasti-Corder internal mixer at 120 °C, with a mixing speed of 30–80 rpm, for 10 min. The obtained results indicate that by adding 2% (weight percentage) of citric acid to the TPS mixtures, there is an improvement in the physical–mechanical properties, as well as structural changes that can indicate both cross-linking reactions by esterification in stages and depolymerisation reactions. The sample of TPS plasticized with glycerol, which contains OMMT, shows an increase in tensile strength by 34.4%, compared to the control sample.

Keywords: thermoplastic starch; montmorillonite; citric acid; plasticizer; mechanical properties

check for updates

Citation: Stelescu, M.D.; Oprea, O.-C.; Sonmez, M.; Ficai, A.; Motelica, L.; Ficai, D.; Georgescu, M.; Gurau, D.F. Structural and Thermal Characterization of Some Thermoplastic Starch Mixtures. *Polysaccharides* **2024**, *5*, 504–522. https://doi.org/10.3390/polysaccharides5040032

Academic Editor: Janusz Kapusniak

Received: 5 August 2024
Revised: 16 September 2024
Accepted: 19 September 2024
Published: 24 September 2024

Copyright: © 2024 by the authors. Licensee MDPI, Basel, Switzerland. This article is an open access article distributed under the terms and conditions of the Creative Commons Attribution (CC BY) license (https://creativecommons.org/licenses/by/4.0/).

1. Introduction

In recent years, the development of new biodegradable materials that can partially or totally replace synthetic polymers in certain applications has been pursued [1–4]. These types of materials are generally based on natural polymers and have several advantages, as follows: they are biodegradable, non-toxic, have a low cost, are renewable, do not affect the environment, etc. [5,6]. Among these, materials based on thermoplastic starch (TPS) are completely biodegradable and are already used to obtain packaging, in agriculture, the food industry, the pharmaceutical industry, medicine and other industries [7,8]. Currently, numerous studies are being carried out regarding the expansion of its use in other fields, through the development of new types of starch-based biodegradable plastic materials with suitable properties for different applications [9,10].

Starch is a reserve polysaccharide, specific to plant organisms, which is found both in photosynthetic tissues and in most reserve tissues (seeds, tubers, etc.). It is a semi-crystalline polymer that is made up of amylose and amylopectin (Figure S1). Amylose constitutes approximately 15–30% of starch, does not form a gel if hot water is added, and is less soluble in water but can be completely hydrolysed by the enzymes α-amylase and β-amylase. Amylose has a straight chain structure (Figure S1a), generated by α 1–4 glycosidic bonds, that has about 300–7000 glucose units and a molecular mass of approximately 1×10^5–1×10^6 Da [8,11].

Amylopectin is a highly branched polymer that makes up about 70–85% of starch. Amylopectin has both α 1–4 glycosidic bonds and α 1–6 glycosidic bonds that are formed at the branching points (Figure S1b). It has about 2000–200,000 glucose units and a molecular mass of about 1×10^7–1×10^9 Da. Amylopectin is soluble in water, forms a gel when hot water is added and cannot be completely hydrolysed with the α-amylase and β-amylase enzymes [11,12]. Depending on the content of amylose and amylopectin, the characteristics of starch, such as water absorption capacity, gelatinization, retrogradation and swelling in different humidity and temperature conditions, are different. For this reason, most starches used in food or industrial applications are modified to obtain the desired properties [13–15].

In the native starch, a large number of hydrogen bonds are formed, creating strong intermolecular connections. For these reasons, in order to obtain a starch mixture with thermoplastic properties, it is necessary to change the internal crystalline structure of the starch molecule, by breaking these hydrogen bonds. Thus, to reduce the melting temperature of starch and obtain starch-based mixtures with thermoplastic properties, several types of plasticizers are currently used. Starch, in the presence of plasticizers, at high temperatures (90 °C–180 °C), is gelatinized to form a viscous suspension, a process that leads to the decomposition of the granular material [8,15]. At the same time, the melting temperature of the starch is reduced, so that at high temperatures and shear forces, it can be processed by methods specific to thermoplastic materials.

Adding plasticizers plays a very important role because they can form hydrogen bonds with the starch, replacing the strong interaction between the molecular hydroxyl groups of the starch, thus transforming it into a material with thermoplastic properties. This type of plasticized starch is called thermoplastic starch (TPS). In addition to the well-known plasticizers, the literature also reports some less common substances, such as deep eutectic solvents (DESs) [16], plasticizers with amide groups (urea and formamide) [17], sugars [18] or phosphazenes [19]. Among the most used plasticizers used for this purpose, we mention glycerine and sorbitol. Glycerol (propane-1,2,3-triol), commonly known as glycerine, is a viscous, colourless, sweet, odourless liquid, soluble in water and alcohol, with a boiling point of 290 °C. Glycerol hardly evaporates and freezes, it is hygroscopic and absorbs water vapour from the atmosphere until an equilibrium is established. Sorbitol (with the chemical formula $C_6H_{14}O_6$), also known as glucitol, is a sweet-tasting polyol that can be obtained following the reduction of glucose, by transforming the aldehyde group into a hydroxyl group. It has a melting point of 95 °C and a boiling point of 296 °C. Both glycerol and sorbitol can destroy starch granules to form an amorphous structure [20–22].

In addition to the advantages presented above, most TPS-based materials also present some disadvantages, such as poor mechanical properties, sensitivity to moisture, high water vapour permeability, poor processing properties (due to high viscosity and reduced flow in the melt), the change in properties due to the process of starch degradation, etc. [23,24].

One of the methods analysed in several papers to improve the mechanical properties, thermal stability and water resistance of TPS consists in adding a small amount (below 5% by weight) of the nanoclay montmorillonite (MMT) [25–27]. MMT is actually a natural layered aluminosilicate (from the clay group) of type 2:1, meaning that it has two tetrahedral sheets of silica sandwiching a central octahedral sheet of alumina. To improve the properties, a good dispersion of MMT in the TPS matrix with the formation of interfacial bonds is necessary. In organically modified montmorillonite clay (OMMT), the spaces between the MMT layers are enlarged by replacing the original inorganic cations in the layer galleries with organic cations. There are several methods of obtaining polymer nanocomposites based on OMMT (by in situ polymerisation, by solution intercalation or melt intercalation, etc.), but the melt intercalation method is the most ecological, economical and more adapted to the conditions and existing requirements in the plastics and rubber industry [28,29].

Several scientific studies [30,31] have shown that the addition of citric acid to TPS mixtures leads to the improvement of the affinity between starch and the other ingredients during the thermo-mechanical processing of the mixture. Citric acid (2-hydroxy-1,2,3-propane tricarboxylic acid $C_6H_8O_7$) is a tricarboxylic acid that appears as a colourless powder with

a sour taste, easily soluble in water. Citric acid can react with starch through esterification reactions that lead both to the formation of cross-linking bonds between the starch chains and to a partial depolymerisation of the starch [20,30,31]. Additionally, by adding citric acid, the granular structure of the starch is modified, and in this way, the mechanical properties of TPS can be improved.

Most of the plasticized starch compositions reported in the literature [32,33] were manufactured by conventional solution casting procedures. Therefore, such procedures imply multiple operations on technological flow, with large water consumption and long required times. By contrast, in the present research, the TPS is obtained by using an internal mixer, in which starch gelatinization takes place when plasticizers are added at ~120 °C. The test samples were obtained by compression moulding (a plastic material-specific obtaining method), using specific moulds and the laboratory electrical press. As a consequence, the obtaining time is reduced, the water need is eliminated and the technological flow has fewer steps. In obtaining the mixtures, the starch was plasticized with glycerine or with a mixture of glycerine and sorbitol. The influence of the introduction of citric acid, the OMMT nanofiller and an additive (siloxane polymer) on the structure, mechanical and thermal properties was analysed. The obtained results were compared with other literature reports for TPS with similar compositions made by the solution casting technique.

2. Materials and Methods

2.1. Materials

Upon obtaining TPS samples, soluble starch obtained from potatoes (with a high content of amylopectin) and two types of plasticizers, namely glycerine and sorbitol, were used. At the same time, citric acid was used as a compatibilizing agent, as well as a montmorillonite clay nanofiller and an additive—Genioplast—to improve the processing properties. The materials used to obtain the nanocomposites are presented in Table 1.

Table 1. The materials used and their characteristics.

No.	Material	Producer	Role	Characteristics
1	Soluble starch obtained from potatoes	Lach-Ner, Neratovice Czech Republic	Polymer matrix	Substance insoluble in water 0.28%, loss on drying (at 105 °C) 17.52%
2	Glycerin	Lach-Ner	Plasticizer	Acidity 0.02%, density 1.26 g/cm^3
3	Sorbitol	Thermo Scientific, Czech Republic	Plasticizer	D-Sorbitol 97%
4	Anhydrous citric acid	Reanal Laborvegyszer Kft., Budapest, Hungary	Compatibility agent	$C_8H_8O_7$, molecular mass of 192.13 g/mol, purity 99.8%, 9.8%, sulphate ash < 0.02%, chlorides (Cl) < 0.0005%, sulphates (SO_4) < 0.02%, oxalates (C_2O_4) < 0.05%
5	Nanoclay, surface modified, Nanomer 31PS	Sigma-Aldrich, St. Louis, MA, USA	Nanofiller	Contains 0.5–5 wt.% aminopropyl-triethoxysilane, 15–35 wt.% octadecyl-amine, matrix: montmorillonite clay base material, size < 20 micron
6	Genioplast Pellet P Plus	Wacker Chemie AG, Munich, Germany	Additive	Ultrahigh molecular weight siloxane polymer 70% and fumed silica 30%

2.2. Obtaining the Samples

The starch gelatinization process took place in the internal mixer Brabender Plasti-Corder internal mixer 350E (Duisburg, Germany), as reported in [34,35]. The processing parameters were as follows: temperature of 120 °C, mixing time of 10 min, and mixing speed of 30 rpm in the first 3 min and then 80 rpm in the next 7 min. Before use, starch was dried in the oven for 24 h at 80 °C to reduce its moisture content. The ingredients were weighed according to the formulations, and the mixer was loaded up to 75–80%. They

were mixed for 5–7 min in a Berzelius beaker and then in the Brabender Plasti-Corder internal mixer, where the gelatinization phenomenon took place and the TPS samples were obtained.

Table 2 shows the compositions of the obtained mixtures. The ratio of starch and plasticizers were chosen to form two separate series, namely as follows: for mixtures S1–S4, the starch/glycerine ratio is 70:30, and for mixtures S5–S8, the starch/glycerine/sorbitol ratio is 60:20:20. Other preliminary tests made for the optimization of the compositions indicated that lower plasticizer quantities leads to stiff samples that will crack and break too easily. At the same time, larger plasticizer amounts will lead to difficult mixing, with a tendency to generate lumps and stick to the mixer, with no proper blending being achieved.

Table 2. Formulations and sample codes.

Ingredients	Sample Code							
	S1	**S2**	**S3**	**S4**	**S5**	**S6**	**S7**	**S8**
Starch (g)	70	70	70	70	60	60	60	60
Glycerine (g)	30	30	30	30	20	20	20	20
Sorbitol (g)	-	-	-	-	20	20	20	20
Citric acid (g)	-	2	2	2	-	2	2	2
OMMT (g)	-	-	2.1	2.1	-	-	1.8	1.8
Genioplast (g)				2.1				1.8

Using the Brabender Mixer WinMix software, version 3.2.30, the variations in the torque and the temperature recorded during the obtaining of the samples can be seen (Figure 1). One can observe the moment of gelatinization, when the torque reached a maximum, but also the efficient mixing of the components, as when the torque exhibited low variations. This method of highlighting the gelatinization process is different from the standardized one, because, in general, plasticized starch is obtained in aqueous solutions at certain concentrations, and gelation characteristics were analysed using the Brabender Amylograph following the standard programme [32,36]. The diagrams presented in Figure 1 confirm the above observations. Therefore, in the first 3 min, at a rotation speed of 30 rpm, the ingredients were heated to the temperature of the mixer, starch granules were intimately mixed with plasticizers (glycerine, sorbitol), starch granules swelled and the gelatinization process began. In this process, starch granules broke down, hydrogen bonds broke and, as a result, the viscosity of the mixtures increased, as indicated by the torque increase (Figure 1). Plasticizer was absorbed faster in the starch granules of the mixture with a lower amount of plasticizer (sample S2), and the gelatinization process occurred faster than for the mixture containing a higher amount of plasticizer (sample S7). In the following minutes, the rotation speed increased to 80 rpm and an increase in torque can be seen up to a maximum, indicating an increase in viscosity as a result of a greater number of hydrogen bonds breaking. Starch granules underwent the gelatinization process, which led to starch solubilisation and resulted in plasticized starch (TPS). A decrease in viscosity was then noticed (indicated by a decrease in torque) due to the melting of the crystalline regions of starch [36,37]. The maximum torque and values obtained at the end of the mixing operation for sample S2 are higher than those corresponding to sample S7, due to the different content of plasticizers, which led to different viscosities of samples during processing. The temperature in the mixer chamber decreased after the introduction of the ingredients that were at room temperature, but increased over time both due to the temperature in the mixing chamber and due to the friction and shearing forces, which changed with the increase in the rotation speed from 30 rpm to 80 rpm (Figure 1).

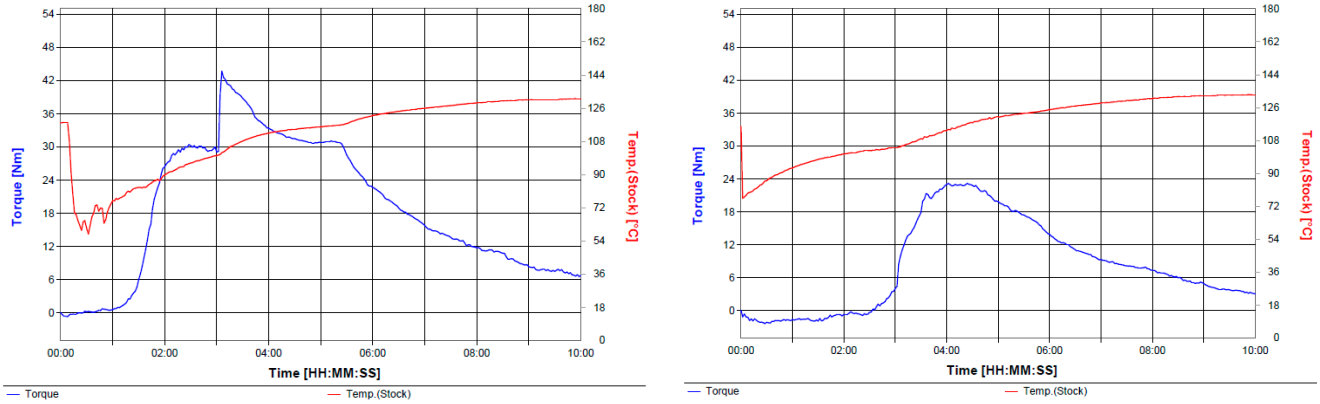


Figure 1. Diagrams showing the variations in the torque and the temperature versus time, when obtaining the mixtures using the Brabender Plasti-Corder.

Obtaining Test Specimens

The obtained mixtures were used to prepare compression moulded plates with dimensions of 150 × 150 × 2 mm^3 and 50 × 50 × 6 mm^3, respectively. The Fontijne laboratory press, model TP/600 (manufactured by Fontijne Grotnes, Vlaardingen, The Netherlands) and frame/flash mould were used. Working parameters were as follows: moulding temperature: 140 °C, preheating time: 3 min, preheating pressure: contact, full pressure: 5 MPa, full pressure time: 3 min, cooling time: 10 min, cooling pressure: 5 MPa and cooling temperature: 40 °C (cooling speed of ca. 10 °C/min). From compression moulded plates, the test specimens for determining the properties were obtained by punching, using an automatic punch.

2.3. Material Characterization (FTIR and TG/DSC)

Fourier Transform Infrared (FTIR) spectra of all the samples were taken with a Nicolet IS50 FT-IR spectrometer (Thermo Scientific, Waltham, MA, USA) in the wavenumber range of 4000–400 cm^{-1}, using attenuated total reflection (ATR). IR spectra were collected at a spectral resolution of 4 cm^{-1} over 32 scans. For evaluating the short-range ordered structure of starch samples, the spectra were processed by deconvolution using OMNIC software (version 9.1.27). The FTIR 2D maps were recorded with a Nicolet iN10 MX microscope (Nicolet, Waltham, MA, USA).

A STA 449 C Jupiter equipment from Netzsch (Netzsch, Selb, Germany) was used for the thermogravimetric analysis coupled with differential scanning calorimetry (TG/DSC). The samples (~20 mg) were placed in an open Al_2O_3 crucible and heated up at a 10 °C·min^{-1} rate until 900 °C in a dynamic atmosphere (flow of 50 mL·min^{-1} of dried air).

2.4. Physicochemical Characterization

Hardness of samples was measured using a hardener tester, on the Shore A scale and D scale, according to ISO 868 [38]. Samples of 6 mm thickness were used for determinations, a minimum of 5 hardness measurements were taken in different positions of the test specimen, and an average value was determined.

Tensile strength tests were carried out with a Schopper strength tester with a testing speed of 500 mm/min, using dumb-bell-shaped specimens—type IV with a thickness of 2 mm, according to ASTM-D638-14 [39]. Five determinations were made, and the arithmetic mean of all values obtained was calculated.

3. Results and Discussion

3.1. FTIR Spectroscopy and Microscopy

By adding citric acid, the granular structure of the starch is modified, and in this way, the mechanical properties of TPS can be improved. In Figure 2, a mechanism of

the cross-linking reaction of starch in the presence of citric acid through esterification reactions is proposed. At the temperature required to obtain TPS, citric acid dehydrates and forms citric anhydride (**1**). This reacts with the hydroxyl groups in starch to form starch acetate (Figure 2). It is known that starch contains two types of hydroxyl groups, primary (6-OH) and secondary (2-OH and 3-OH) (Figure 2), which are able to react with multifunctional reagents, resulting in cross-linked starches. Due to its linear polysaccharide structure, amylose is much more susceptible to undergo chemical transformations, unlike amylopectin, a polysaccharide with a branched structure, with less-accessible reactive groups. From these considerations, it is assumed that the reaction with citric acid takes place in a higher percentage at the primary hydroxyl groups in the C-6 position of the anhydroglucose ring on the amylose chains and, in a lower percentage, at the hydroxyl groups blocked in the (1–6)-α glycosidic bonds of the amylopectin branches. The reaction between starch and citric acid can take place in several stages. They consist first of an attachment of citric acid through an esterification reaction with the hydroxyl group (**2**), and its further reaction, also through an esterification process, with another hydroxyl group of the starch, thus leading to the formation of cross-linking bonds and the formation of starch citrate (**3**) (Figure 2). The thermal stability of starch citrate depends on the amylopectin content and the starch structure. Thus, according to existing studies, starch citrate with a higher amylopectin content may be more thermally stable than one with a lower content [30].

In addition to these cross-linking reactions, it was observed that by adding citric acid to obtain TPS, a partial depolymerisation between C1 and the glycosidic oxygen in starch can be achieved [30]. Figure 3 presents a mechanism of the hydrolysis reaction of starch with citric acid that leads to the reduction in the molecular mass of starch. This acid hydrolysis is assumed to occur at the glycosidic bonds and is induced by the residual moisture that is available in excess in the starch. In the presence of citric acid, the glycosidic oxygen is protonated and the resulting glycosyl is further hydrolysed by water molecules to form a stable product [30].

Figure 4 shows the spectra for the mixtures of starch plasticized with glycerine (samples S1–S4), and Figure 5 shows the FTIR spectra of the samples of starch plasticized with glycerine and sorbitol (samples S5–S8).

Analysing the FTIR spectra of samples S1–S8, a broad band at 3296–3301 cm^{-1} is observed corresponding to the stretching vibration of the O-H bond associated through hydrogen bonds and the vibrations of the polar O-H bonds of amylose, amylopectin, glycerol, sorbitol and absorbed water, respectively [40]. The absorption bands that appear at 2860–2960 cm^{-1}, 1461–1462 cm^{-1} and 1368–1372 cm^{-1} are due to the stretching vibration of the C-H bonds, to the deformation vibrations of the methylene groups (-CH_2-) and to the symmetric deformation vibration of the methyl groups (-CH_3), respectively [41,42]. The peak at 1366–1369 cm^{-1} can assigned to the branches existing in amylopectin (dimethyl, trimethyl or tert-butyl). The intense absorption bands characteristic of the vibrations of the C-O polar bonds in alcohols, ethers and esters (νC-O) located in the fingerprint region appear in the interval 1040–1250 cm^{-1}. Among them, several absorption bands are assigned to C-O bond stretching vibrations in C–O–H (1148–1151 and 1076–1078 cm^{-1}) and in C-O-C (995–997 cm^{-1}, 853–858 cm^{-1} and 758–761 cm^{-1}) of the anhydroglucose ring of the starch structure [43,44].

The band at 925–926 cm^{-1} is attributed to C–O–C α-1,4-glycosidic and α-1,6-glycosidic stretching [45–47]. Paluch et al. [45] showed that the band in the region of 920–938 cm^{-1} is derived from oscillations of α-1,4-glycosidic and α-1,6-glycosidic bonds. For starch that contains a greater number of C–O–C type bonds coming from α-1,6-glycosidic amylopectin, this band is shifted to higher values of the wavenumber, and for starch with a lower percentage of amylopectin, the band appears at lower values of the wavenumber. They also specified the fact that after the plasticization process, the α-1,6-glycosidic bonds are broken and, therefore, the position of this band appears at lower values of the wavenumber.

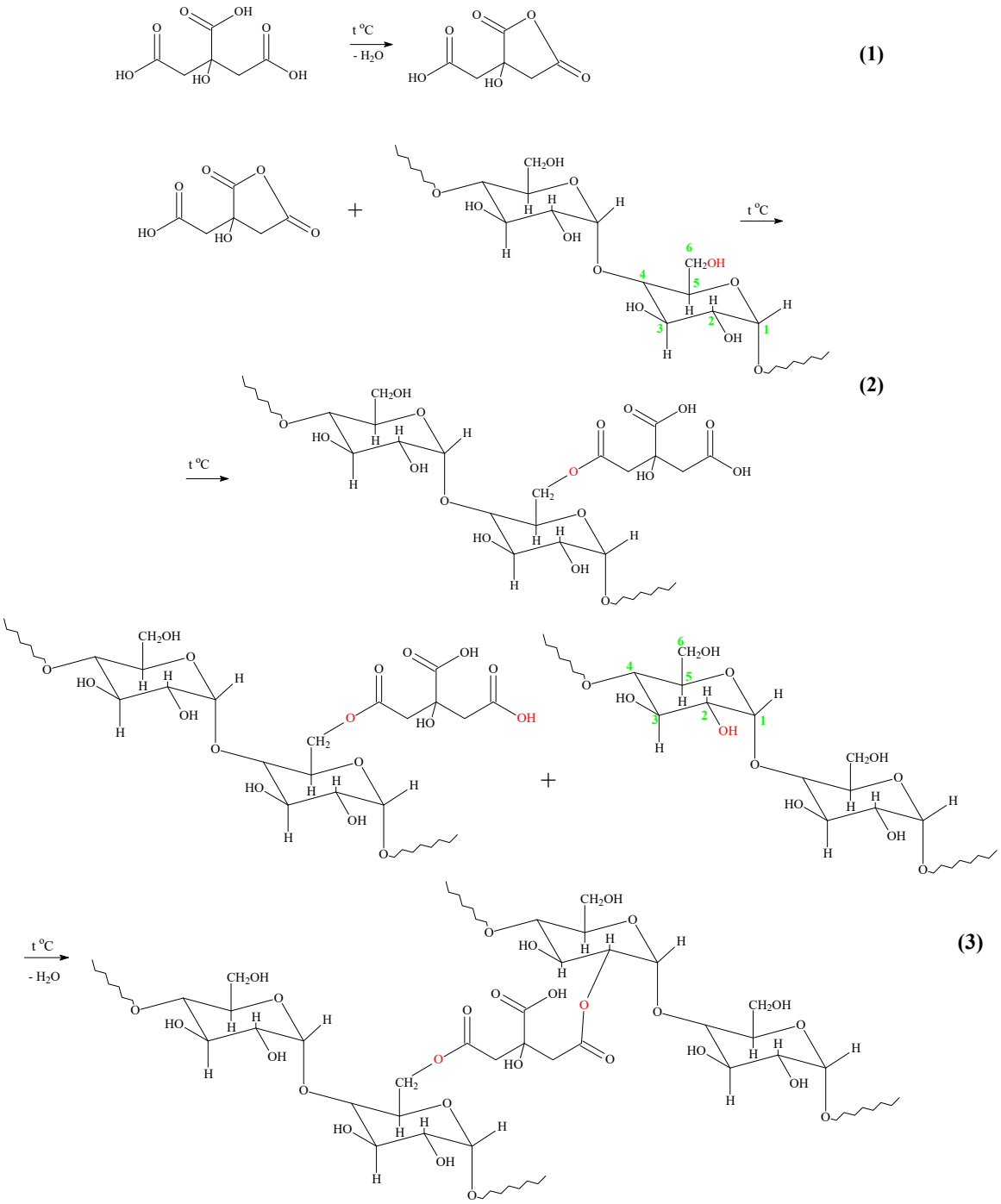


Figure 2. The proposed mechanism of cross-linking of citric acid with starch; green numbers represent the carbon numbering: citric anhydride formation (**1**); esterification reaction between citric anhydride and starch (**2**); formation of starch citrate by cross-linking (**3**).

The samples containing citric acid show a band at ~1722 cm^{-1} specific to the ester bond (R-COO-R), but which has a very low intensity. This could indicate the effectiveness of the citric acid cross-linking of plasticized starch. At the same time, it is also observed that the hydrogen bonds between starch and the plasticizer (glycerol, sorbitol) were improved by the presence of citric acid (the intensity of the peak at 3300 cm^{-1} increases in S2 compared to S1 by approx. 2.1%, and for S6 it increases by 17.6% compared to S5). Seligra et al. [48] and Shi et al. [49] showed that the relationship between the intensity ratio of the hydroxyl group (-OH) at 3300 cm^{-1} (I_{3300}) and that of the peak at 1150 cm^{-1} that is attributed to the C–O

stretch in the C–OH group (I_{1150}) can be used to identify the ester group of starch chains with citric acid. Table 3 shows the peak intensities of specific functional groups and their calculated ratios. It can be observed that the ratios between the peak intensities (I_{3300}/I_{1150}) for the mixtures containing citric acid are lower than those of the mixtures without citric acid. Thus, the I_{3300}/I_{1150} values for mixtures S2, S3 and S4 decrease compared to that of mixture S1, as well as, for mixtures S6, S7 and S8, the ratios decrease compared to the value of the ratio obtained for mixture S5. The reduction in the intensity ratio is related to a lower amount of -OH groups in the citric acid-modified starch mixtures, as a result of the reaction of the -COOH groups with the OH group of starch and glycerine and sorbitol, respectively, by esterification [48–50].

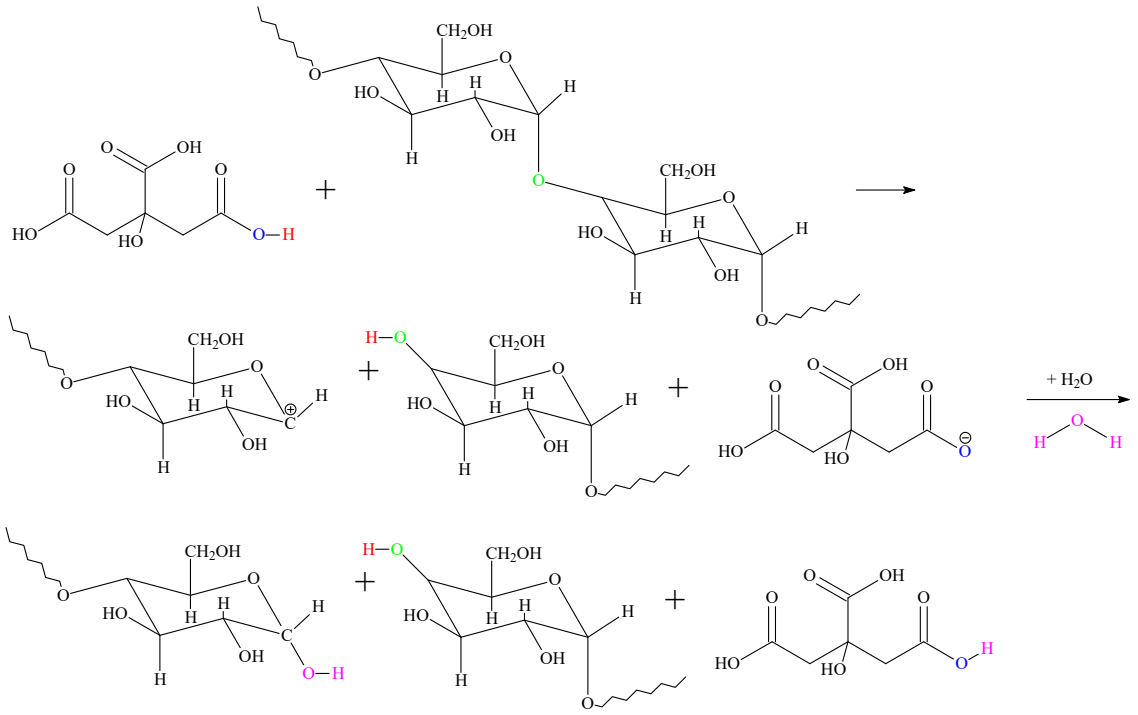
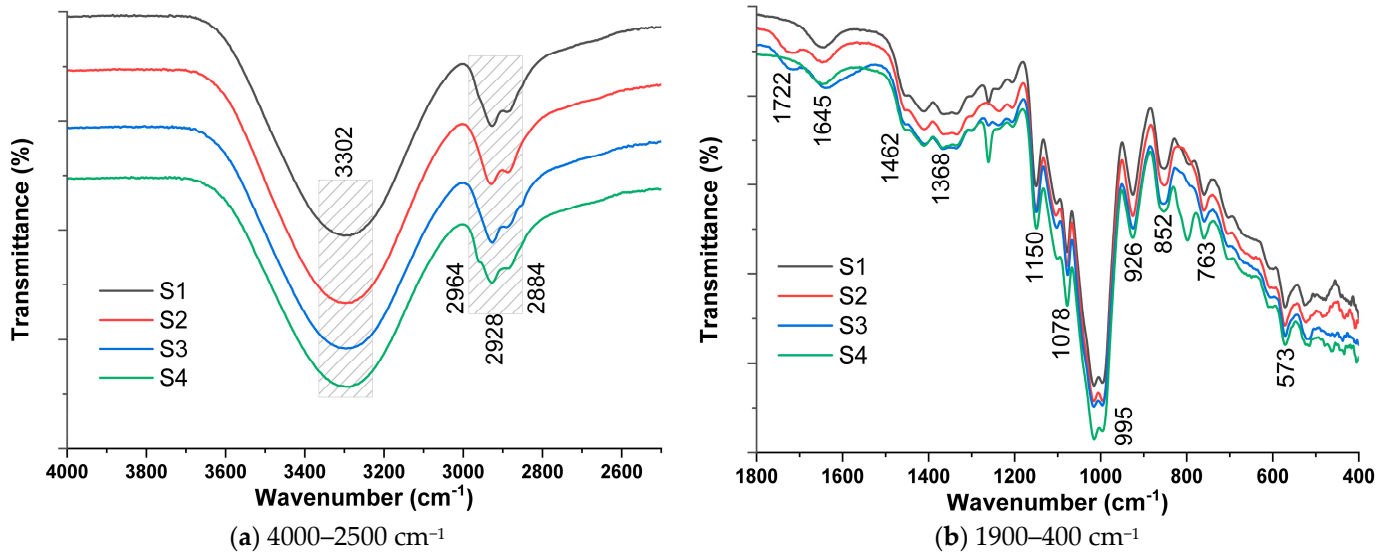
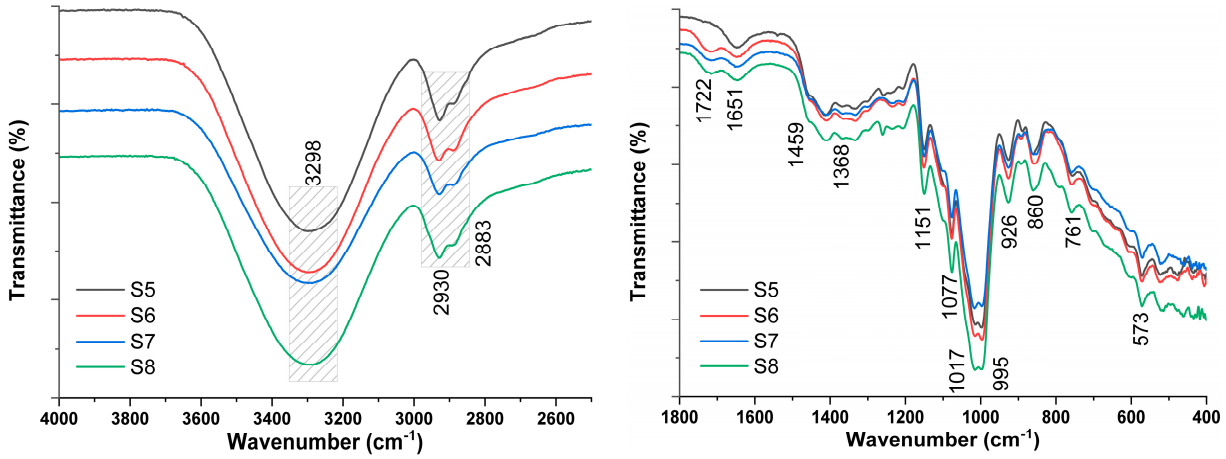


Figure 3. Possible starch hydrolysis reaction with citric acid.



(**a**) 4000–2500 cm^{-1} (**b**) 1900–400 cm^{-1}

Figure 4. FTIR spectra of samples S1–S4.



(**a**) 4000–2500 cm^{-1} (**b**) 1900–400 cm^{-1}

Figure 5. FTIR spectra of samples S5–S8.

Table 3. Values of peak intensity ratios ($I_{3300/I1150}$, $I_{1022/I995}$, $I_{1044/I1022}$) for analysed mixtures.

Sample	$I_{3300/I1150}$	$I_{1022/I995}$	$I_{1044/I1022}$
S1	1.054	1.2163	0.9668
S2	1.013	1.0654	0.7222
S3	1.049	1.0645	0.7229
S4	0.930	1.1853	0.9079
S5	1.301	1.1526	1.1606
S6	1.233	0.9400	0.7655
S7	1.186	0.8224	1.0003
S8	1.230	0.7906	0.9176

Mixtures containing Genioplast ultrahigh molecular weight siloxane polymer (S4 and S8) may contain absorption bands due to ultrahigh molecular weight siloxane polymer at 1373 cm^{-1} (CH) def, at 1019 cm^{-1} (Si-O) str, at 1264 (s) cm^{-1} (Si-CH_3) ((-CH) sym def, at 800 cm^{-1} (Si-C) str; however, they have a low intensity and overlap with other bands [51].

Amylose and amylopectin associate with each other through hydrogen bonds and are arranged radially in layers to form the starch granule. The starch granule is presented as an amorphous matrix in which crystalline areas are scattered. The crystalline areas are made up of short linear chains of amylopectin, which contain about 15–25 glucose units, grouped in the form of a parallel double helix. Amylose forms most of the amorphous regions, which are randomly distributed between the amylopectin clusters. The branching regions are made up of the amorphous layer that separates the crystallites from each other [8]. The bands in the region 1100–900 cm^{-1} are sensitive to the changes in the structure of starch. Several authors [52–54] showed the fact that the IR absorption band at 1042–1049 cm^{-1} is sensitive to the amount of crystalline starch, and the band at 1015–1022 cm^{-1} is influenced by the amount of amorphous starch, and it is caused by the formation of hydrogen bonds between plasticizers and starch. The band from 994–1000 cm^{-1} indicates intramolecular hydrogen bonds of the hydroxyl group from C-6, which are sensitive to hydration, and it is more pronounced in the higher crystalline samples [55]. This led to the use of the intensity ratio for these bands in several studies [56,57], to evaluate changes in the ordered molecular structure over short distances. It was observed that the ratio between the intensity of the band at 1022 cm^{-1} and that of the band at 995 cm^{-1} (I_{1022}/I_{995}) provides information on crystallinity and hydration. Thus, some studies have suggested that changes in the I_{1022}/I_{995} ratio upon hydration of crystalline starch are the result of a nematic–smectic transition [56,57].

For these reasons, to study the effect of ingredient interaction and gelatinization on the amorphous and crystalline structures of the starch used, the spectral region 900–1100 cm^{-1}

was analysed. Since this region included several overlapping bands, their deconvolution was performed using the OMNIC software. Two absorption band intensity ratios were calculated, namely I_{1022}/I_{995} and I_{1044}/I_{1022} cm^{-1} (Table 3), which could provide information regarding the order in the more crystalline regions and, respectively, the state of organization of the double helices located inside the crystallites [57]. From the data presented in Table 3, it can be seen that the most significant changes in the two ratios occur by introducing citric acid in the TPS samples. In these samples, a decrease in the I_{1022}/I_{995} ratio can be observed, which may be due to the increase in the weight of intramolecular H bonds of the hydroxyl group from C6. These could contribute to improving the compatibility between starch and plasticizer, obtaining mixtures with a more homogeneous structure, and favouring the hydration of crystalline starch through nematic–smectic transitions [55]. At the same time, after the introduction of citric acid, a decrease in the I_{1044}/I_{1022} ratio is observed, which indicates a decrease in the weight of the ordered crystalline phase in the samples. So, it can be assumed that by adding citric acid, changes occur that may indicate a more advanced hydration of the crystalline phase of the starch as a result of some nematic–smectic transitions [53]. Our results are consistent with those reported in other works [55,57].

For FTIR microscopy, we have chosen the 2D maps at three wavenumbers: 2929 cm^{-1} assigned to C-H stretching from CH_2 moieties, 1150 cm^{-1} attributed to the C–O stretch in the C–OH and 1015 cm^{-1} assigned to the hydrogen bond formation between plasticizers and starch. The micrographs are presented for samples S1–S4 in Figure 6 and for samples S5–S8 in Figure 7.

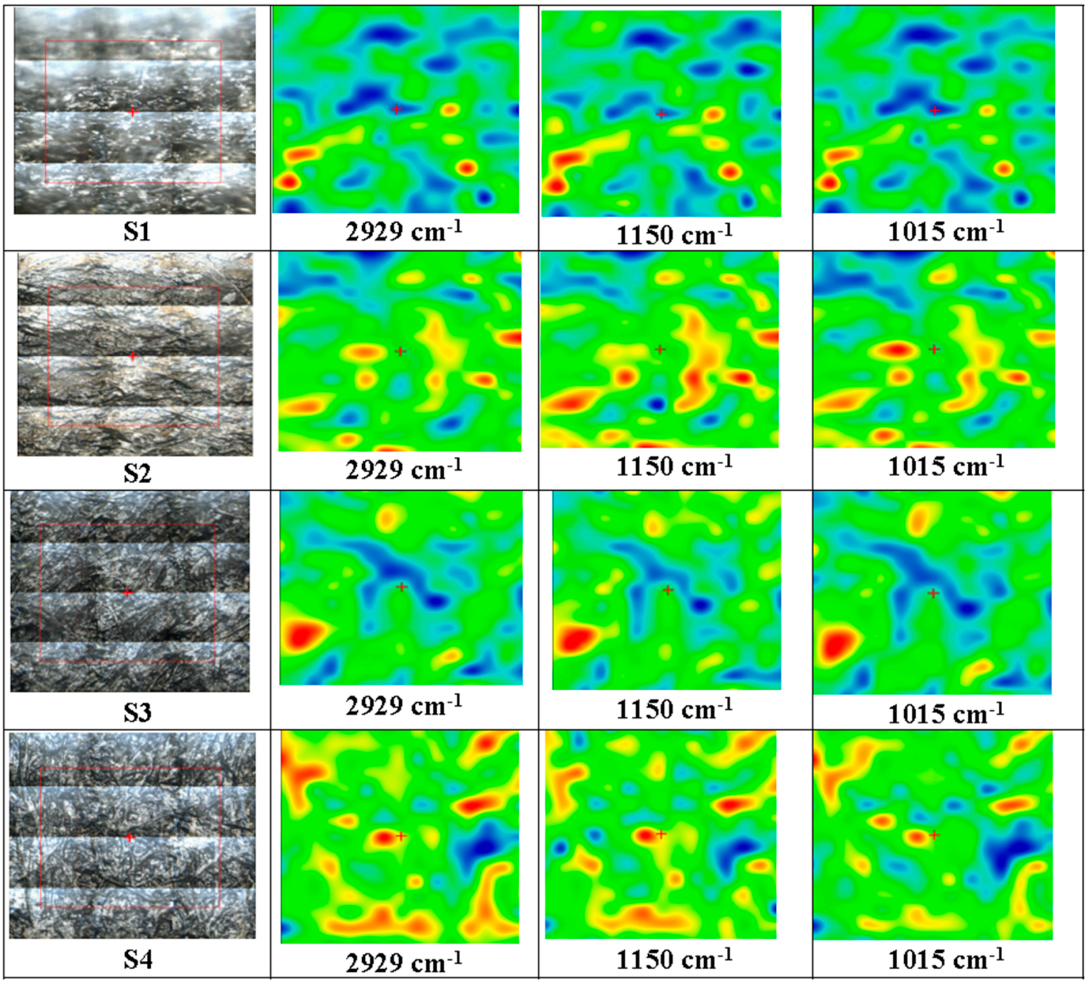


Figure 6. FTIR maps of samples S1–S4 (red areas indicate the highest absorbance, while blue areas correspond to the lowest absorbance).

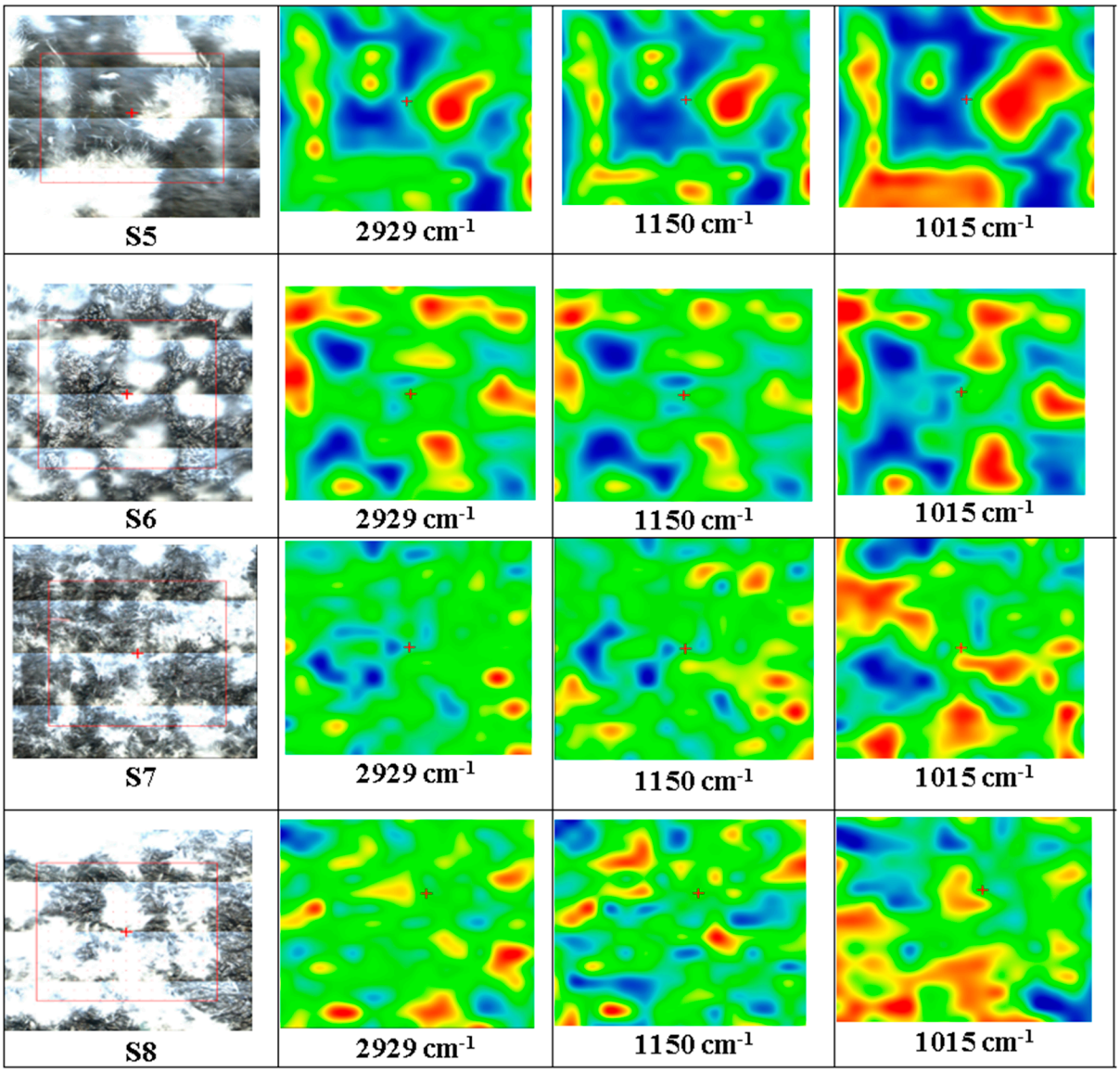


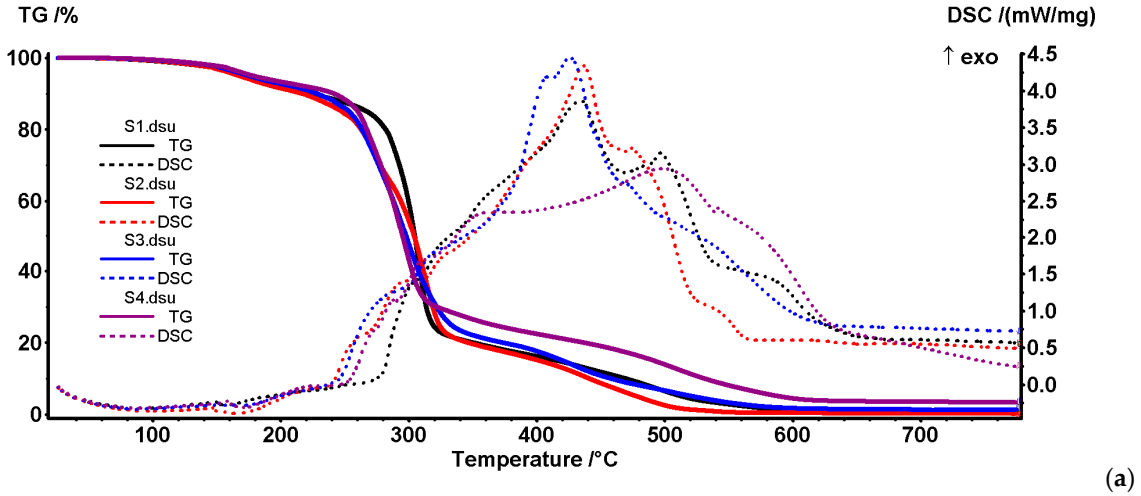
Figure 7. FTIR maps of samples S5–S8 (red areas indicate the highest absorbance, while blue areas correspond to the lowest absorbance).

The blue zones correspond to the regions with lower absorbance and the red zones correspond to higher absorbance regions. For all samples, we can observe a good homogeneity, but there is a clear difference between the S1–S4 series vs. the S5–S8 series. The introduction of sorbitol as a plasticizer negatively influences the sample homogeneity, with the apparition of small, micrometre size, cluster agglomerations being favoured.

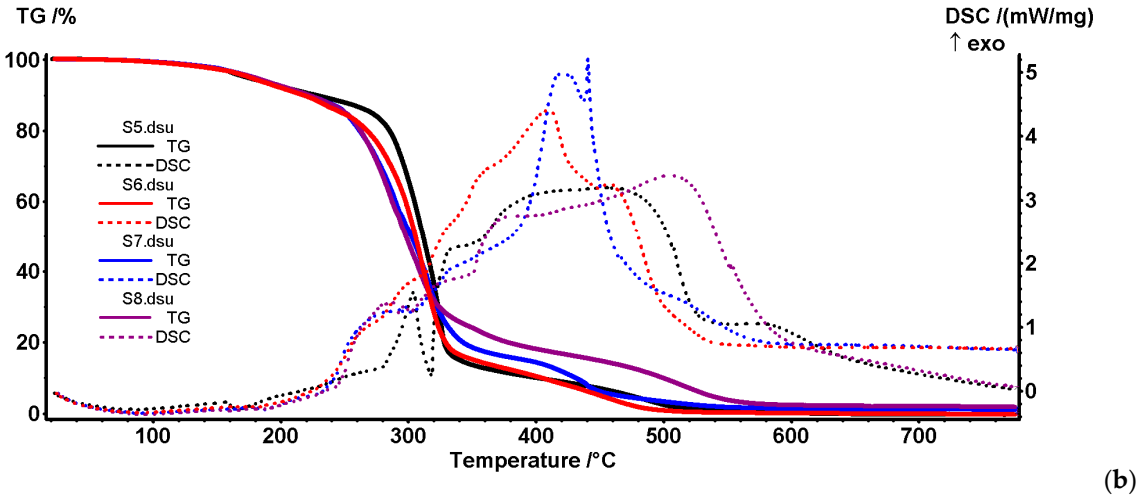
3.2. Thermal Analyses

The TG and DSC curves for all samples up to 900 °C are presented in Figure 8. The first endothermic effect takes place between 90 and 100 °C for the S1–S4 samples and between 88 and 92 °C for the S5–S8 samples and corresponds to the elimination of water humidity from the TPS mass. Samples containing citric acid exhibit an increase in the temperature at which water is eliminated when compared to the S1 and S5 samples, indicating that cross-linking by citric acid makes the water elimination more difficult [58]. After the elimination of humidity up to 140 °C, the samples continue to lose mass slowly until ~250 °C, when the principal mass loss event occurs. The main oxidative degradative process takes place after 250 °C, and is generated by a complex process (Figure S2); on one hand, the fragmentation of the polymeric backbone occurs, and on the other hand, the oxidation of smaller molecular

mass fragments happens. The complexity of the degradation mechanism can be deduced from the multiple shoulders and peaks on the DTG curves (Figure S2 and Table 4). The oxidation process is predominant, as indicated by the overall exothermic effect on the DSC curve. After 320 °C, the carbonaceous residual mass is slowly burned away, as indicated by the strong, broad and asymmetric exothermic effect, with multiple peaks in the region of 400–600 °C. The higher residual mass obtained for the samples S3–S4 and S7–S8 is due to the presence of inorganic fillers (OMMT and SiO_2 generated by Genioplast).



(**a**)



(**b**)

Figure 8. TG-DSC curves of samples S1–S4 (**a**) and S5–S8 (**b**).

The most important numerical data are presented in Table 4. Analysing these data, some conclusions can be drawn. The temperatures $T_{5\%}$ (corresponding to 5% mass loss) and $T_{10\%}$ present different variations for the S1–S4 and S5–S8 series. For the S1–S4 series, the addition of citric acid leads to a small decrease in the $T_{5\%}$ and $T_{10\%}$ (~5–8 °C), most probably due to acid-induced structure fragmentation. The successive addition of fillers, OMMT and Genioplast, leads to an increased thermal stability (~11–25 °C). This effect of inorganic filler on thermal stability was reported before [41,42]; these particles act as an adsorbing energy shield. A somewhat similar but diminished effect can be noticed for $T_{10\%}$ for the S5–S8 samples. After an initial decrease of 9 °C from S5 to S6 due to the addition of citric acid, the stability increase induced by fillers is modest, of 3–4 °C, for the S7 and S8 samples. This can be an indication of some agglomeration of the fillers, but can also be due to a higher content of plasticizers. In the case of $T_{5\%}$ for the S5–S8 samples, a slow increase in stability can be observed (~2–5 °C).

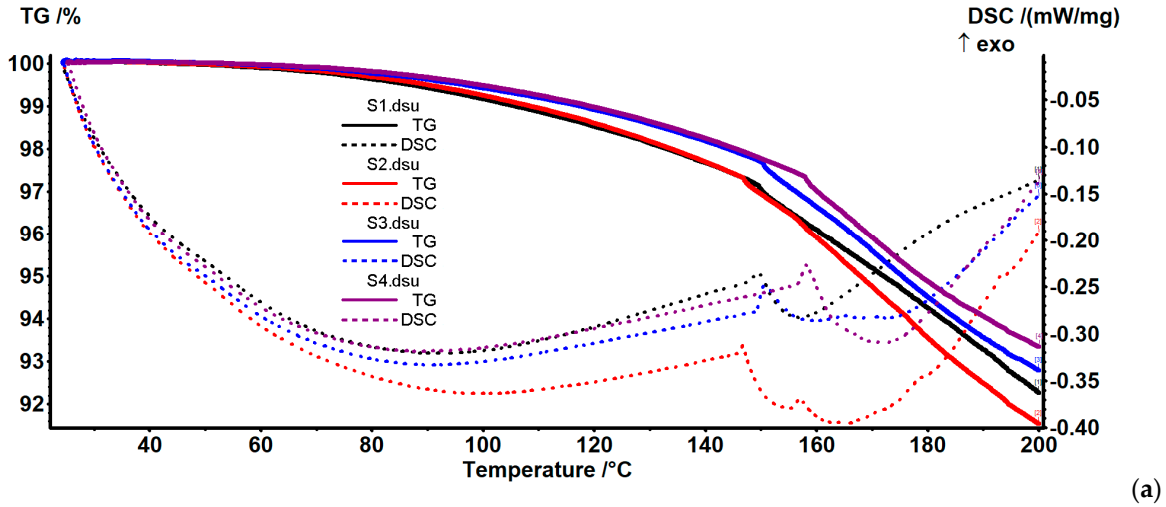
Table 4. Principal numerical data from thermal analysis of S1–S8 samples.

Sample	$T_{5\%}$	$T_{10\%}$	Inflection	Δm (250 °C)	Endo	Exo	DTG Peak (°C)
S1	173 °C	225 °C	149.8 °C	12.42%	156.9 °C	434.7 °C	288.7sh/308.2
S2	168 °C	217 °C	147.1 °C	15.58%	155.5/165.4 °C	436.3 °C	272.6/312.8
S3	175 °C	228 °C	150.7 °C	14.00%	159.7/172.4 °C	426.4 °C	263.8sh/302.0
S4	179 °C	242 °C	158.2 °C	11.63%	172.8 °C	499.3 °C	266.3/290.1/296.9
S5	174 °C	227 °C	156.6 °C	12.08%	166.8 °C	452.3 °C	291.6/321.1
S6	176 °C	218 °C	162.9 °C	15.46%	168.2/181.4 °C	410.6 °C	298.7/308.8
S7	179 °C	221 °C	153.6 °C	14.76%	160.4/186.4 °C	418.8 °C	289.4/310.2/316.2
S8	179 °C	222 °C	151.7 °C	14.80%	157.4/179.6 °C	505.5 °C	286.0/294.1/308.6

The mass loss up to 250 °C increases for S2 and S6 samples when compared to the S1 or S5, respectively. This is related to the presence of citric acid, which generates a partial hydrolysis of starch (Figure 3), with the fragments being easier to degrade. The presence of fillers OMMT and Genioplast leads further to a smaller mass loss, as the inorganic part will not degrade, but also as it acts as anchoring points for smaller fragments, slowing the degradation process. The S7 and S8 samples with larger plasticizer amounts will also present a larger mass loss compared to the S3 and S4 samples.

The DTG curve indicates the temperatures at which the maximum mass loss rate occurs (due to decomposition and oxidation). For both series, the samples with OMMT and Genioplast present the maximum mass loss rate on the DTG curve under 300 °C, despite an initial better thermal stability.

The detailed information for the temperature interval 20–200 °C is presented in Figure 9. The most important feature is the inflection point in the region 150–160 °C, which separates two different mass loss events. At lower temperatures, the absorbed water molecules (residual humidity) are eliminated, while at higher temperatures, a more complex degradation occurs, as indicated by the multiple endothermic effects on the DSC curves. This second event is mostly generated by the elimination of structural water molecules from the starch and the breaking of the hydrogen bonds between starch and plasticizers [30]. Similar inflection points are presented in other reports [30]. The sorbitol addition in the S5 sample leads to an increase in the inflection temperature point, from 149.8 to 156.6 °C, due to increasing intermolecular hydrogen bonds that trap the water molecules [30].



(**a**)

Figure 9. *Cont.*

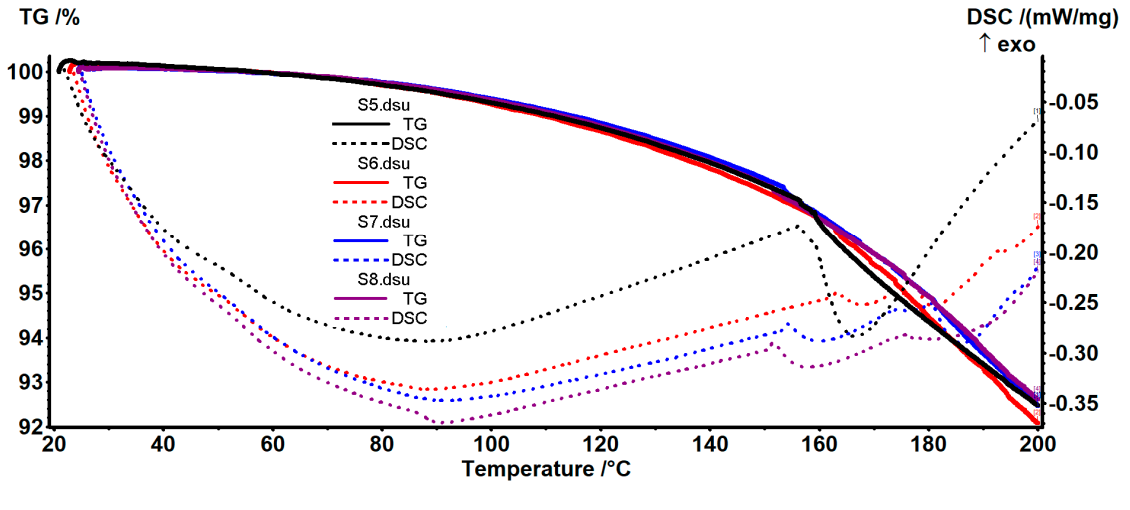


Figure 9. Detail of TG-DSC curves of samples S1–S4 (**a**) and S5–S8 (**b**).

3.3. Physical–Mechanical Properties

TPS retrogradation is a complex phenomenon that consists in the reorganization (recrystallization) of starch macromolecules (amylose and amylopectin). This recrystallization occurs at a high speed in the case of amylose and at a much slower speed in the case of amylopectin. Crystal formation is accompanied by an increase in rigidity and a separation of the polymer/solvent phases [59,60]. To eliminate the retrogradation, there is a need for chemical, physical or enzymatic modifications of the starch, the use of different types of plasticizers or the addition of some ingredients (such as nanowires or other thermoplastic materials) to improve these properties [60,61]. For the obtained plasticized starch samples S1–S8, the physical–mechanical characteristics are presented in Table 5.

Table 5. Physical–mechanical characteristics of plasticized starch samples.

Sample Code	Hardness	Hardness	Tensile Strength	Elongation at Break
	° ShA	° ShD	N/mm^2	%
S1	97 ± 0.577	46 ± 0.577	2.64 ± 0.096	140 ± 6.666
S2	96 ± 0.577	43 ± 0.577	5.17 ± 0.01	120 ± 11.547
S3	91 ± 0.577	32 ± 0.577	6.95 ± 0.186	60 ± 6.666
S4	87 ± 0.882	34 ± 0.577	2.84 ± 0.1	100 ± 5.773
S5	93 ± 0.577	39 ± 0.577	2.37 ± 0.255	100 ± 6.666
S6	90 ± 0.577	31 ± 0.577	4.21 ± 0.041	40 ± 4.409
S7	88 ± 0.577	29 ± 0.577	4.24 ± 0.035	40 ± 6.666
S8	86 ± 0.882	33 ± 0.577	4.22 ± 0.045	60 ± 6.666

The results show that the samples plasticized with glycerine and sorbitol have a lower hardness than those plasticized only with glycerine, the hardness differences being 0–6° ShA and 1–7° ShD, respectively. This aspect can be explained by the fact that the samples containing both sorbitol and glycerine have a higher plasticizer content. The fact that the average values of the tensile strength are better for the S1–S4 mixtures (with a smaller amount of plasticizer) compared to the S5–S8 mixtures can be explained in the same way. The values of these characteristics are comparable to those obtained by other researchers [32,33,62,63], who used conventional TPS-obtaining methods. It can be seen from Table 6 that the reported values were not greatly influenced by the obtaining method, but are rather dependent on the starch/plasticizer ratio and the starch origin or plasticizer type.

Table 6. Mechanical properties values reported in the literature.

Starch Type	Plasticizer	Obtaining Method	Tensile Strength N/mm^2	Elongation at Break, %	Ref.
Corn starch	glycerol (30% *w*/*w*)	Solution casting	2.53	40	[32]
Corn starch	glycerol, sorbitol 1:1 (30% *w*/*w*)	Solution casting	5.74	55	[32]
Corn starch	glycerol, sorbitol 1:1 (45% *w*/*w*)	Solution casting	2.8	70	[32]
Sugar palm starch	glycerol, sorbitol 1:1 (45% *w*/*w*)	Solution casting	3.99	39	[62]
Sugar palm starch	glycerol (30% *w*/*w*)	Solution casting	2.5	61.6	[62]
Potato starch	glycerol (33% *w*/*w*)	Solution casting	3.05	70	[63]
Rice starch	glycerol (33% *w*/*w*)	Solution casting	1.8	49	[63]
Potato starch	glycerol (30% *w*/*w*)	Solution casting	2.42	46.6	[33]

The samples containing citric acid (samples S2 and S6/S2–S4, and S6–S8, respectively) have better values of tensile strength compared to the control samples (S1 and S5, respectively), while hardness is a few degrees lower; this can be due to a better homogenization of the mixtures through the introduction of citric acid as a compatibilizing agent, as well as due to the partial depolymerisation of starch [20]. A more significant improvement (95.8% for tensile strength) was observed for the sample plasticized only with glycerine (S2 compared to S1).

Depending on the strength of the interfacial interactions between the polymer matrix and MMT, three types of nanocomposites can be formed, namely the following: (1) intercalated nanocomposites for which the polymer matrix is inserted into the layered silicate structure in a crystallographic, regular way; (2) flocculated nanocomposites that have structures identical to the intercalated ones, but the silicate layers are sometimes flocculated due to the interactions of the hydroxylated ends of the silicate layers; (3) exfoliated nanocomposites for which the individual layers of clay are separated inside the polymer matrix, with a distance between the layers that depends on the degree of clay loading [27,64,65]. To obtain intercalated or exfoliated polymer nanocomposites that lead to an improvement in properties, we have added an organically modified montmorillonite clay (OMMT) in the samples S3, S4, S7 and S8. As in the OMMT, the spaces between the layers are enlarged; higher molecular weight polymers might enter the clay galleries. Some studies have shown that for TPS/OMMT nanocomposites, only the plasticizer (glycerol) can effectively intercalate between the OMMT layers, and starch macromolecules can be more difficult to intercalate. Nevertheless, different compatibilizing agents, such as citric acid, can improve both TPS plasticity and OMMT dispersion in the TPS matrix [65–67].

When adding the OMMT nanoarray (samples S3 and S7/S3–S4 and S7–S8), a decrease in hardness can be observed of 2–5° ShA and 2–11° ShD, respectively, which could indicate a change in the morphology of the samples. For the samples plasticized only with glycerine, an improvement in the tensile strength by 34.4% was observed, which may indicate the formation of an intercalated or exfoliated nanocomposite that led to the improvement of mixture properties [68]. This is in agreement with other published works that emphasized the fact that clay would interact preferentially with glycerol because it has a lower molecular mass. In addition, it was observed that for mixtures plasticized only with glycerol, the temperature at which the gelation process takes place is higher and, therefore, the morphology and characteristics of the TPS are different from those of TPS in which there are two types of plasticizers (Figure 2) [60].

For the samples containing the Genioplast additive, hardness changes of approx. 2–5° ShA and 2–4° ShD, respectively, can be noticed, which can be determined by both the improvement in processing properties and by the reduction of the crystalline phase through the addition of polymer siloxane.

The values of elongation at break are small, 40–140%, for all samples and are in agreement with the results obtained by other researchers [32,62,63]. These values can be

influenced by the existence of chemical or physical cross-links, by the reinforcement with OMMT that restricts the mobility of the polymers, by the proportion of the crystalline and amorphous phase, etc.

Thermoplastic mixtures based on starch and plasticizer do not have good mechanical properties (aspect confirmed by other works [68,69]), but by adding citric acid and OMMT, an improvement in tensile strength is observed, and the hardness decreases by max 6° ShA. These aspects may indicate that in the control mixtures (S1 and S5, respectively), there may be residual starch granules in the amorphous matrix of amylase and amylopectin, which increased the stiffness of the mixtures by creating some physical cross-links. When adding citric acid and the other ingredients, it is possible that the amount of starch granules is reduced, thus reducing the hardness of the mixtures and leading to an improvement of the other characteristics [67].

4. Conclusions

The thermoplastic starch mixtures made, both those based on starch and glycerine (in a mass ratio of 70:30) and those based on starch, glycerine and sorbitol (in a mass ratio of 60:20:20), do not present good mechanical properties, but with the addition of citric acid and the OMMT nanofiller, an improvement in the tensile strength is observed, while the hardness decreases by max 6° ShA. FTIR analyses show that by adding 2% (mass percentage) citric acid in TPS mixtures, cross-linking reactions can take place through stepwise esterification and depolymerisation reactions, as well as a more advanced hydration of the crystalline phase of the starch due to some nematic–smectic transitions, with reduced structural order. Further studies on the introduction of obtained TPS mixtures in food packaging, biodegradable polymeric blends, 3D printing filaments, etc. can determine the domains in which such blends can be used.

Supplementary Materials: The following supporting information can be downloaded at: https://www.mdpi.com/article/10.3390/polysaccharides5040032/s1, Figure S1: Chemical structure of amylose (a) and amylopectin (b); Figure S2: The thermal analysis curves (TG, DTG and DSC) for samples S1–S8.

Author Contributions: Conceptualization and methodology, M.D.S. and M.S.; composite preparation, M.S., D.F.G., M.D.S. and M.G.; investigation, M.S., D.F., L.M., O.-C.O., D.F.G., M.D.S., A.F. and M.G.; writing—original draft preparation, D.F.G., M.D.S., L.M. and O.-C.O.; writing—review and editing, D.F., A.F., M.S. and M.G. All authors have read and agreed to the published version of the manuscript.

Funding: This work was supported by a grant of the Ministry of Research, Innovation, and Digitization, CCCDI—UEFISCDI, project number PN-III-P2-2.1-PED-2021-3177; 712PED/2022 "Valorificarea superioara a polietilenei reciclate prin compoundare cu amidon modificat chimic si nanopulberi in vederea obtinerii de materiale cu proprietati antimicrobiene pentru imprimante 3D RepRap". The authors are grateful to the Romanian Government for providing access to the research infrastructure of the National Center for Micro and Nanomaterials through the National Program titled "Installations and Strategic Objectives of National Interest".

Institutional Review Board Statement: Not applicable.

Informed Consent Statement: Not applicable.

Data Availability Statement: The data presented in this study are available upon request from the corresponding authors.

Conflicts of Interest: The authors declare no conflicts of interest.

References

1. Motelica, L.; Ficai, D.; Oprea, O.C.; Ficai, A.; Ene, V.L.; Vasile, B.S.; Andronescu, E.; Holban, A.M. Antibacterial Biodegradable Films Based on Alginate with Silver Nanoparticles and Lemongrass Essential Oil-Innovative Packaging for Cheese. *Nanomaterials* **2021**, *11*, 2377. [CrossRef] [PubMed]
2. Athanasopoulou, E.; Bigi, F.; Maurizzi, E.; Karellou, E.I.E.; Pappas, C.S.; Quartieri, A.; Tsironi, T. Synthesis and characterization of polysaccharide- and protein-based edible films and application as packaging materials for fresh fish fillets. *Sci. Rep.* **2024**, *14*, 517. [CrossRef] [PubMed]

3. Agarwal, S. Major factors affecting the characteristics of starch based biopolymer films. *Eur. Polym. J.* **2021**, *160*, 110788. [CrossRef]
4. Cernencu, A.; Lungu, A.; Stancu, I.C.; Vasile, E.; Iovu, H. Polysaccharide-Based 3D Printing Inks Supplemented with Additives. *Univ. Politeh. Buchar.* **2019**, *81*, 175–186.
5. Motelica, L.; Ficai, D.; Oprea, O.; Ficai, A.; Trusca, R.D.; Andronescu, E.; Holban, A.M. Biodegradable Alginate Films with ZnO Nanoparticles and Citronella Essential Oil-A Novel Antimicrobial Structure. *Pharmaceutics* **2021**, *13*, 1020. [CrossRef]
6. Onyeaka, H.; Obileke, K.; Makaka, G.; Nwokolo, N. Current Research and Applications of Starch-Based Biodegradable Films for Food Packaging. *Polymer* **2022**, *14*, 1126. [CrossRef]
7. Motelica, L.; Ficai, D.; Ficai, A.; Oprea, O.C.; Kaya, D.A.; Andronescu, E. Biodegradable Antimicrobial Food Packaging: Trends and Perspectives. *Foods* **2020**, *9*, 1438. [CrossRef]
8. Stelescu, M.D.; Oprea, O.C.; Motelica, L.; Ficai, A.; Trusca, R.D.; Sonmez, M.; Nituica, M.; Georgescu, M. Obtaining and Characterizing New Types of Materials Based on Low-Density Polyethylene and Thermoplastic Starch. *J. Compos. Sci.* **2024**, *8*, 134. [CrossRef]
9. Siqueira, L.D.; Arias, C.I.L.; Maniglia, B.C.; Tadini, C.C. Starch-based biodegradable plastics: Methods of production, challenges and future perspectives. *Curr. Opin. Food Sci.* **2021**, *38*, 122–130. [CrossRef]
10. Adewale, P.; Yancheshmeh, M.S.; Lam, E. Starch modification for non-food, industrial applications: Market intelligence and critical review. *Carbohyd. Polym.* **2022**, *291*, 119590. [CrossRef]
11. Jobling, S. Improving starch for food and industrial applications. *Curr. Opin. Plant Biol.* **2004**, *7*, 210–218. [CrossRef] [PubMed]
12. Compart, J.; Singh, A.; Fettke, J.; Apriyanto, A. Customizing Starch Properties: A Review of Starch Modifications and Their Applications. *Polymer-* **2023**, *15*, 3491. [CrossRef] [PubMed]
13. Agarwal, S.; Singhal, S.; Godiya, C.B.; Kumar, S. Prospects and Applications of Starch based Biopolymers. *Int. J. Environ. an Ch* **2023**, *103*, 6907–6926. [CrossRef]
14. Caldonazo, A.; Almeida, S.L.; Bonetti, A.F.; Lazo, R.E.L.; Mengarda, M.; Murakami, F.S. Pharmaceutical applications of starch nanoparticles: A scoping review. *Int. J. Biol. Macromol.* **2021**, *181*, 697–704. [CrossRef]
15. Le Corre, D.; Bras, J.; Dufresne, A. Starch Nanoparticles: A Review. *Biomacromolecules* **2010**, *11*, 1139–1153. [CrossRef]
16. Skowronska, D.; Wilpiszewska, K. Deep Eutectic Solvents for Starch Treatment. *Polymers* **2022**, *14*, 220. [CrossRef]
17. Montilla-Buitrago, C.E.; Gómez-López, R.A.; Solanilla-Duque, J.F.; Serna-Cock, L.; Villada-Castillo, H.S. Effect of Plasticizers on Properties, Retrogradation, and Processing of Extrusion-Obtained Thermoplastic Starch: A Review. *Starch-Starke* **2021**, *73*, 2100060. [CrossRef]
18. Alee, M.; Duan, Q.F.; Chen, Y.; Liu, H.S.; Ali, A.; Zhu, J.; Jiang, T.Y.; Rahaman, A.; Chen, L.; Yu, L. Plasticization Efficiency and Characteristics of Monosaccharides, Disaccharides, and Low-Molecular-Weight Polysaccharides for Starch-Based Materials. *ACS Sustain. Chem. Eng.* **2021**, *9*, 11960–11969. [CrossRef]
19. Nykänen, V.P.S.; Härkönen, O.; Nykänen, A.; Hiekkataipale, P.; Ruokolainen, J.; Ikkala, O. An efficient and stable star-shaped plasticizer for starch: Cyclic phosphazene with hydrogen bonding aminoethoxy ethanol side chains. *Green. Chem.* **2014**, *16*, 4339–4350. [CrossRef]
20. Wang, N.; Yu, J.G.; Ma, X.F.; Wu, Y. The influence of citric acid on the properties of thermoplastic starch/linear low-density polyethylene blends. *Carbohyd. Polym.* **2007**, *67*, 446–453.
21. Carvalho, A.J.F.; Zambon, M.D.; Curvelo, A.A.D.; Gandini, A. Thermoplastic starch modification during melt processing: Hydrolysis catalyzed by carboxylic acids. *Carbohyd. Polym.* **2005**, *62*, 387–390. [CrossRef]
22. Moscicki, L.; Mitrus, M.; Wójtowicz, A.; Oniszczuk, T.; Rejak, A.; Janssen, L. Application of extrusion-cooking for processing of thermoplastic starch (TPS). *Food Res. Int.* **2012**, *47*, 291–299. [CrossRef]
23. Bangar, S.P.; Whiteside, W.S.; Ashogbon, A.O.; Kumar, M. Recent advances in thermoplastic starches for food packaging: A review. *Food Packag. Shelf* **2021**, *30*, 100743. [CrossRef]
24. Liu, H.S.; Xie, F.W.; Yu, L.; Chen, L.; Li, L. Thermal processing of starch-based polymers. *Prog. Polym. Sci.* **2009**, *34*, 1348–1368. [CrossRef]
25. Müller, C.M.O.; Laurindo, J.B.; Yamashita, F. Composites of thermoplastic starch and nanoclays produced by extrusion and thermopressing. *Carbohyd. Polym.* **2012**, *89*, 504–510. [CrossRef]
26. De Azeredo, H.M.C. Nanocomposites for food packaging applications. *Food Res. Int.* **2009**, *42*, 1240–1253. [CrossRef]
27. Aouada, F.A.; Mattoso, L.H.C.; Longo, E. New strategies in the preparation of exfoliated thermoplastic starch-montmorillonite nanocomposites. *Ind. Crop Prod.* **2011**, *34*, 1502–1508. [CrossRef]
28. Paul, D.R.; Robeson, L.M. Polymer nanotechnology: Nanocomposites. *Polymer* **2008**, *49*, 3187–3204. [CrossRef]
29. Picard, E.; Vermogen, A.; Gerard, J.F.; Espuche, E. Barrier properties of nylon 6-montmorillonite nanocomposite membranes prepared by melt blending: Influence of the clay content and dispersion state—Consequences on modelling. *J. Membr. Sci.* **2007**, *292*, 133–144. [CrossRef]
30. Chi, Y.; Maitland, E.; Pascall, M.A. The effect of citric acid concentrations on the mechanical, thermal, and structural properties of starch edible films. *Int. J. Food Sci. Technol.* **2024**, *59*, 1801–1813. [CrossRef]
31. Tharanathan, R.N. Starch-value addition by modification. *Crit. Rev. Food Sci.* **2005**, *45*, 371–384. [CrossRef] [PubMed]
32. Hazrol, M.D.; Sapuan, S.M.; Zainudin, E.S.; Zuhri, M.Y.M.; Wahab, N.I.A. Corn Starch (*Zea mays*) Biopolymer Plastic Reaction in Combination with Sorbitol and Glycerol. *Polymers* **2021**, *13*, 242. [CrossRef] [PubMed]

33. Tarique, J.; Sapuan, S.M.; Khalina, A. Effect of glycerol plasticizer loading on the physical, mechanical, thermal, and barrier properties of arrowroot (*Maranta arundinacea*) starch biopolymers. *Sci. Rep.* **2021**, *11*, 13900. [CrossRef] [PubMed]
34. Kazemi, A.; Khorasani, S.N.; Dinari, M.; Khalili, S. Mechanical and barrier properties of LLDPE/TPS/OMMT packaging film in the presence of POE-g-IA or POE-g-MA. *J. Polym. Res.* **2021**, *28*, 133. [CrossRef]
35. Nituica, M.; Oprea, O.; Stelescu, M.D.; Sonmez, M.; Georgescu, M.; Alexandrescu, L.; Motelica, L. Polymeric Biocomposite Based on Thermoplastic Polyurethane (TPU) and Protein and Elastomeric Waste Mixture. *Materials* **2023**, *16*, 5279. [CrossRef]
36. Adamczyk, G.; Krystyjan, M.; Kuzniar, P.; Kowalczewski, P.L.; Bobel, I. An Insight into Pasting and Rheological Behavior of Potato Starch Pastes and Gels with Whole and Ground Chia Seeds. *Gels* **2022**, *8*, 598. [CrossRef]
37. Balet, S.; Guelpa, A.; Fox, G.; Manley, M. Rapid Visco Analyser (RVA) as a Tool for Measuring Starch-Related Physiochemical Properties in Cereals: A Review. *Food Anal. Method.* **2019**, *12*, 2344–2360. [CrossRef]
38. *ISO 868*; Plastics and Ebonite—Determination of Indentation Hardness by Means of a Durometer (Shore Hardness). ISO: Geneva, Switzerland, 2003. Available online: https://standards.iteh.ai/catalog/standards/sist/b00a2780-f641-4857-8bb1-eb0d574b4af3/iso-868-2003 (accessed on 5 March 2024).
39. *ASTM-D638-14*; Standard Test Method for Tensile Properties of Plastics. ASTM International: West Conshohocken, PA, USA, 2015. Available online: https://cdn.standards.iteh.ai/samples/90583/526a83abb7544d49ac1a1a36382859fe/ASTM-D638-14.pdf (accessed on 1 August 2024).
40. Fonseca-García, A.; Osorio, B.H.; Aguirre-Loredo, R.Y.; Calambas, H.L.; Caicedo, C. Miscibility study of thermoplastic starch/polylactic acid blends: Thermal and superficial properties. *Carbohyd. Polym.* **2022**, *293*, 119744. [CrossRef]
41. Caicedo, C.; Pulgarin, H.L.C. Study of the Physical and Mechanical Properties of Thermoplastic Starch/Poly(Lactic Acid) Blends Modified with Acid Agents. *Processes* **2021**, *9*, 578. [CrossRef]
42. Motelica, L.; Ficai, D.; Oprea, O.C.; Trusca, R.D.; Ficai, A.; Stelescu, M.D.; Sonmez, M.; Nituica, M.; Mustatea, G.; Holban, A.M. Antimicrobial Packaging for Plum Tomatoes Based on ZnO Modified Low-Density Polyethylene. *Int. J. Mol. Sci.* **2024**, *25*, 6073. [CrossRef]
43. Kizil, R.; Irudayaraj, J.; Seetharaman, K. Characterization of irradiated starches by using FT-Raman and FTIR spectroscopy. *J. Agr. Food Chem.* **2002**, *50*, 3912–3918. [CrossRef] [PubMed]
44. Mano, J.F.; Koniarova, D.; Reis, R.L. Thermal properties of thermoplastic starch/synthetic polymer blends with potential biomedical applicability. *J. Mater. Sci. Mater. Med.* **2003**, *14*, 127–135. [CrossRef] [PubMed]
45. Paluch, M.; Ostrowska, J.; Tynski, P.; Sadurski, W.; Konkol, M. Structural and Thermal Properties of Starch Plasticized with Glycerol/Urea Mixture. *J. Polym. Environ.* **2022**, *30*, 728–740. [CrossRef]
46. Sankri, A.; Arhaliass, A.; Dez, I.; Gaumont, A.C.; Grohens, Y.; Lourdin, D.; Pillin, I.; Rolland-Sabaté, A.; Leroy, E. Thermoplastic starch plasticized by an ionic liquid. *Carbohyd. Polym.* **2010**, *82*, 256–263. [CrossRef]
47. Park, J.W.; Im, S.S.; Kim, S.H.; Kim, Y.H. Biodegradable polymer blends of Poly(L-lactic acid) and gelatinized starch. *Polym. Eng. Sci.* **2000**, *40*, 2539–2550. [CrossRef]
48. Seligra, P.G.; Jaramillo, C.M.; Famá, L.; Goyanes, S. Biodegradable and non-retrogradable eco-films based on starch-glycerol with citric acid as crosslinking agent. *Carbohyd. Polym.* **2016**, *138*, 66–74. [CrossRef]
49. Shi, R.; Zhang, Z.Z.; Liu, Q.Y.; Han, Y.M.; Zhang, L.Q.; Chen, D.F.; Tian, W. Characterization of citric acid/glycerol co-plasticized thermoplastic starch prepared by melt blending. *Carbohyd. Polym.* **2007**, *69*, 748–755. [CrossRef]
50. Sukkaneewat, B.; Panrot, T.; Rojruthai, P.; Wongpreedee, T.; Prapruddivongs, C. Plasticizing effects from citric acid/palm oil combinations for sorbitol-crosslinked starch foams. *Mater. Chem. Phys.* **2022**, *278*, 125732. [CrossRef]
51. Marin, D.C.; Vecchio, A.; Ludueña, L.N.; Fasce, D.; Alvarez, V.A.; Stefani, P.M. Revalorization of Rice Husk Waste as a Source of Cellulose and Silica. *Fiber Polym.* **2015**, *16*, 285–293. [CrossRef]
52. Van Soest, J.J.G.; Tournois, H.; de Wit, D.; Vliegenthart, J.F.G. Short-range structure in (partially) crystalline potato starch determined with attenuated total reflectance Fourier-transform IR spectroscopy. *Carbohyd. Res.* **1995**, *279*, 201–214. [CrossRef]
53. Yang, S.; Dhital, S.; Zhang, M.N.; Wang, J.; Chen, Z.G. Structural, gelatinization, and rheological properties of heat-moisture treated potato starch with added salt and its application in potato starch noodles. *Food Hydrocolloid* **2022**, *131*, 107802. [CrossRef]
54. Gómez-López, R.A.; Montilla-Buitrago, C.E.; Villada-Castillo, H.S.; Sáenz-Galindo, A.; Avalos-Belmontes, F.; Serna-Cock, L. Co-Plasticization of Starch with Glycerol and Isosorbide: Effect on Retrogradation in Thermo-Plastic Cassava Starch Films. *Polymers* **2023**, *15*, 2104. [CrossRef]
55. Capron, I.; Robert, P.; Colonna, P.; Brogly, M.; Planchot, V. Starch in rubbery and glassy states by FTIR spectroscopy. *Carbohyd. Polym.* **2007**, *68*, 249–259. [CrossRef]
56. Warren, F.J.; Gidley, M.J.; Flanagan, B.M. Infrared spectroscopy as a tool to characterise starch ordered structure—A joint FTIR-ATR, NMR, XRD and DSC study. *Carbohyd. Polym.* **2016**, *139*, 35–42. [CrossRef] [PubMed]
57. Nhouchi, Z.; Botosoa, E.P.; Chèné, C.; Karoui, R. Mid infrared as a tool to study the conformational structure of starch and proteins with oil addition during gelatinization. *LWT Food Sci. Technol.* **2022**, *157*, 113093. [CrossRef]
58. Gebresas, G.A.; Szabó, T.; Marossy, K. A comparative study of carboxylic acids on the cross-linking potential of corn starch films. *J. Mol. Struct.* **2023**, *1277*, 134886. [CrossRef]
59. Kohyama, K.; Matsuki, J.; Yasui, T.; Sasaki, T. A differential thermal analysis of the gelatinization and retrogradation of wheat starches with different amylopectin chain lengths. *Carbohyd. Polym.* **2004**, *58*, 71–77. [CrossRef]

60. Lara, S.C.; Salcedo, F. Gelatinization and retrogradation phenomena in starch/montmorillonite nanocomposites plasticized with different glycerol/water ratios. *Carbohyd. Polym.* **2016**, *151*, 206–212. [CrossRef]
61. Arroyo, O.H.; Huneault, M.A.; Favis, B.D.; Bureau, M.N. Processing and Properties of PLA/Thermoplastic Starch/Montmorillonite Nanocomposites. *Polym. Compos.* **2010**, *31*, 114–127. [CrossRef]
62. Sanyang, M.L.; Sapuan, S.M.; Jawaid, M.; Ishak, M.R.; Sahari, J. Effect of Plasticizer Type and Concentration on Tensile, Thermal and Barrier Properties of Biodegradable Films Based on Sugar Palm (*Arenga pinnata*) Starch. *Polymers* **2015**, *7*, 1106–1124. [CrossRef]
63. Zolek-Tryznowska, Z.; Kaluza, A. The Influence of Starch Origin on the Properties of Starch Films: Packaging Performance. *Materials* **2021**, *14*, 1146. [CrossRef] [PubMed]
64. Weiss, J.; Takhistov, P.; McClements, D.J. Functional materials in food nanotechnology. *J. Food Sci.* **2006**, *71*, R107–R116. [CrossRef]
65. Majdzadeh-Ardakani, K.; Navarchian, A.H.; Sadeghi, F. Optimization of mechanical properties of thermoplastic starch/clay nanocomposites. *Carbohyd. Polym.* **2010**, *79*, 547–554. [CrossRef]
66. Zhang, Q.X.; Yu, Z.Z.; Xie, X.L.; Naito, K.; Kagawa, Y. Preparation and crystalline morphology of biodegradable starch/clay nanocomposites. *Polymer* **2007**, *48*, 7193–7200. [CrossRef]
67. Wang, N.; Zhang, X.X.; Han, N.; Bai, S.H. Effect of citric acid and processing on the performance of thermoplastic starch/montmorillonite nanocomposites. *Carbohyd. Polym.* **2009**, *76*, 68–73. [CrossRef]
68. Cyras, V.P.; Manfredi, L.B.; Ton-That, M.T.; Vázquez, A. Physical and mechanical properties of thermoplastic starch/montmorillonite nanocomposite films. *Carbohyd. Polym.* **2008**, *73*, 55–63. [CrossRef]
69. Park, H.M.; Lee, W.K.; Park, C.Y.; Cho, W.J.; Ha, C.S. Environmentally friendly polymer hybrids—Part I—Mechanical, thermal, and barrier properties of thermoplastic starch/clay nanocomposites. *J. Mater. Sci.* **2003**, *38*, 909–915. [CrossRef]

Disclaimer/Publisher's Note: The statements, opinions and data contained in all publications are solely those of the individual author(s) and contributor(s) and not of MDPI and/or the editor(s). MDPI and/or the editor(s) disclaim responsibility for any injury to people or property resulting from any ideas, methods, instructions or products referred to in the content.